

Ionic and electronic transport in $\text{La}_2\text{Ti}_2\text{SiO}_9$ -based materials

Y.V. Pivak, V.V. Kharton*, E.N. Naumovich, J.R. Frade, F.M.B. Marques

Department of Ceramics and Glass Engineering, CICECO, University of Aveiro, 3810-193 Aveiro, Portugal

Received 7 December 2006; received in revised form 6 January 2007; accepted 9 January 2007

Available online 3 February 2007

Abstract

The total conductivity of monoclinic $\text{La}_2\text{Ti}_2\text{SiO}_9$ is mixed oxygen-ionic and n-type electronic, and increases on reduction of the oxygen partial pressure down to 10^{-21} atm at 973–1223 K. The substitution of Ti^{4+} with Nb^{5+} decreases both contributions to the conductivity, whilst Pr doping and reducing $p(\text{O}_2)$ have opposite effects. The oxygen ion transference numbers of $\text{La}_2\text{Ti}_2\text{SiO}_{9-\delta}$, $\text{LaPrTi}_2\text{SiO}_{9\pm\delta}$ and $\text{La}_2\text{Ti}_{1.8}\text{Nb}_{0.2}\text{SiO}_{9\pm\delta}$ ceramics, measured by the faradaic efficiency and e.m.f. methods, vary in the range 0.15–0.32, increasing when temperature decreases. In air, the activation energies for the ionic and electronic transport are 1.23–1.40 and 1.59–1.74 eV, respectively. Protonic contribution to the conductivity in wet atmospheres becomes significant at temperatures below 1000 K. The experimental data and the results of atomistic computer simulations suggest that the oxygen-ionic and electronic transport is primarily determined by processes involving TiO_6 octahedra. The ionic conduction may occur via both the vacancy and interstitial migration mechanisms, but the former is more favorable energetically and should dominate, at least, in reducing atmospheres. The average thermal expansion coefficients of $\text{La}_2\text{Ti}_2\text{SiO}_9$ -based ceramics, calculated from dilatometric data in air, are $(8.7\text{--}9.5) \times 10^{-6} \text{ K}^{-1}$ at 300–1373 K. The lattice of lanthanum titanate-silicate is almost intolerant with respect to *A*-site deficiency and to doping with lower-valence cations, such as Sr and Fe.

© 2007 Elsevier Inc. All rights reserved.

Keywords: Lanthanum titanate-silicate; Oxygen ionic conductivity; n-type electronic transport; Ion transference number; Thermal expansion; Atomistic computer simulations

1. Introduction

Oxygen ion-conducting solid electrolytes are key materials for numerous high-temperature electrochemical devices, such as solid oxide fuel cells (SOFCs) [1,2]. Although possessing a high energy-conversion efficiency, environmental safety and fuel flexibility, the practical application of SOFCs is still limited due to the high cost of the component materials and processing. Development of novel low-cost materials with optimized transport and thermomechanical properties is of vital importance in this field. Recently, considerable attention has been focused on the silicates with apatite-type $A_{10-x}(\text{SiO}_4)_6\text{O}_{2-\delta}$ [3–9] and cuspidine-type $A_4(\text{Si}_2\text{O}_7)\text{O}_{2-\delta}$ [10,11] structures, where the *A* sublattice comprises rare-earth and/or alkaline-earth cations. The essential features of these Si-containing solid electrolytes are the flexibility of the crystal structure,

enabling improvements in transport properties via cation doping, and an important role of the lattice relaxations near diffusing anions [3–11]. Having a relatively high oxygen-ionic conductivity and a moderate thermal expansion [3–11], these may be of a substantial interest when considering the low cost of raw materials and well-developed technologies for SiO_2 -based film processing, used in the electronic industry. On the other hand, despite the great number of silicates where similar structural elements are present in the crystal lattice, and significant ionic conduction may thus be expected, literature data on the correlations between silicate structure and transport properties are scarce. Such information is also critical for the developments of suitable SOFC sealants based on glass-ceramics [12–15], another important challenge for SiO_2 -containing materials. The glass-ceramic seals applied to separate cathode and anode chambers and to maintain the gas-tightness of the system, should exhibit thermo-mechanical and chemical stability and good compatibility with other SOFC components. In terms of electrical

*Corresponding author. Fax: +351 234 425300.

E-mail address: kharton@cv.ua.pt (V.V. Kharton).

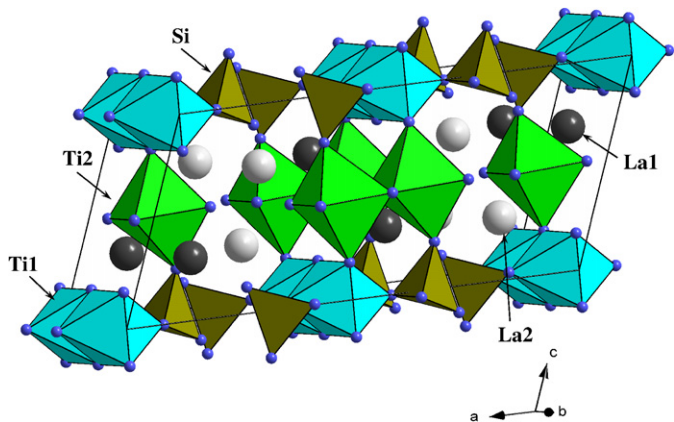


Fig. 1. Crystal structure of $\text{La}_2\text{Ti}_2\text{SiO}_9$.

properties, these glass-ceramics should behave as insulators with total conductivity (σ) lower than 10^{-4} S/cm, in order to avoid parasitic currents decreasing the system efficiency. Due to similar bond energies, the behavior of glassy components is, as a rule, quite similar to that of the parent crystalline phases.

Continuing our research on silicate-based materials for the high-temperature electrochemical applications [8,9], the present work is centered on the study of several compositions within the monoclinic $\text{La}_{2-x}\text{A}_x\text{Ti}_{2-y}\text{B}_y\text{SiO}_{9\pm\delta}$ ($A = \text{Pr, Sr, Y}$; $B = \text{Nb, Fe}$) system. Particular emphasis is given to the phase relationships, total and partial oxygen-ionic conductivities, transference numbers, thermal expansion, and behavior in reducing conditions. The crystal structure of the base compound, $\text{La}_2\text{Ti}_2\text{SiO}_9$ (Fig. 1), includes a network of isolated SiO_4 tetrahedra connected by two types of TiO_6 octahedra. Unlike perovskite-type structures where all octahedra are corner-sharing, the equivalent TiO_6 polyhedra in the $\text{La}_2\text{Ti}_2\text{SiO}_9$ share their edges. Two non-equivalent La sites existing in this structure are located between SiO_4 and TiO_6 units. Also, the lattice comprises relatively large cavities between metal-oxygen polyhedra, which can be occupied by interstitial ions. Possible contributions of oxygen vacancies and interstitials were evaluated incorporating higher- and lower-valence dopants, studying the relationships between transport properties and oxygen partial pressure, and using the atomistic computer simulations.

2. Experimental

Powders of $\text{La}_{2-x}\text{A}_x\text{Ti}_{2-y}\text{B}_y\text{SiO}_{9\pm\delta}$ ($A = \text{Pr, Sr, Y}$; $B = \text{Nb, Fe}$; $x = 0-1$; $y = 0-1$) and $\text{Y}_2\text{Ti}_2\text{SiO}_9$ were prepared from high-purity metal oxides, nitrates and carbonates by the conventional solid-state synthesis route. The reactions were performed at 1173–1473 K for 15–25 h in air, with intermediate re-grinding steps and final ball-milling in ethanol. Then the powders were uniaxially pressed at 100–150 MPa into disks of various thickness; gas-tight ceramics were sintered at 1598–1668 K for 20 h in air. X-ray diffraction (XRD) patterns were collected using

a Rigaku D/MAX-B diffractometer (Bragg-Brentano geometry, $\text{CuK}\alpha$ radiation, 2θ angle range 10–100°, step 0.02°, 9 s/step). The structural parameters were refined using the full-profile Rietveld method, employing FullProf software [16]. In the refinement procedure, the scale factor, zero shift and background parameters, lattice constants, atomic coordinates and fractions, isotropic temperature factors, peak profile and texture parameters were taken into account. A Hitachi S-4100 scanning electron microscope (SEM) with a Rontec UHV detection system for the energy-dispersive spectroscopy (EDS) was used for microstructural analysis. Thermal expansion was studied in air using a Linseis L70 dilatometer (heating rate of 3 K/min). Thermogravimetric analysis (TGA) was carried out using a Setaram SetSys 16/18 instrument (flowing dry air, heating/cooling rate of 3 K/min, dwell at 1473 K for 1 h). The temperature dependencies of total conductivity (σ) in flowing air, O_2 -Ar and 10% H_2 -90% N_2 mixtures were studied by the AC impedance spectroscopy (HP4284A precision LCR meter, 20 Hz–1 MHz); the oxygen partial pressure in the measuring cell was controlled by an yttria-stabilized zirconia (YSZ) oxygen sensor. To estimate possible protonic contributions to the conductivity, the impedance spectra were collected both in dry gas (with the water-vapor partial pressure lower than 10^{-4} atm), and in humidified atmospheres (with $p(\text{H}_2\text{O}) \approx 0.032$ atm). The oxygen ion transference numbers were determined by the modified electromotive force (EMF) and faradaic efficiency (FE) methods [17,18].

The atomic simulations technique using the GULP software [19] is well known in literature (e.g. [20]). This approach is based on the Born model for ionic solids, where the charge of ions is assigned to their formal oxidation state. The interactions between the ions are formulated in terms of long-range electrostatic (Coulombic) forces and short-range Pauli repulsion and van der Waals dispersion, modeled using a standard Buckingham potential:

$$V_{ij} = A_{ij} \exp\left(-\frac{r_{ij}}{\rho_{ij}}\right) - C_{ij}r^{-6}, \quad (1)$$

where A_{ij} , ρ_{ij} and C_{ij} are potential parameters and r_{ij} is the distance between two ions. The polarizability caused by the presence of charged defects in the lattice is taken into account by means of the shell model [21], treating each ion in terms of heavy core (representing the nucleus and core electrons) connected via one harmonic spring to a shell (representing the outer electrons). The defect modelling is performed using a Mott-Littleton approach [22]; the crystal around a defect is partitioned into the inner spherical region with explicit description of atomic relaxations, and the outer region extended to infinity, where the defect-lattice interactions are relatively weak and can be treated by approximate quasi-continuum methods. The short-range potential and shell model parameters, including the three-body potential for SiO_4 units, were selected from

Download English Version:

<https://daneshyari.com/en/article/1333281>

Download Persian Version:

<https://daneshyari.com/article/1333281>

[Daneshyari.com](https://daneshyari.com)